

CONFIDENTIAL

Copy 5  
RM E51C22

MAY 11 1951



# RESEARCH MEMORANDUM

INVESTIGATION OF OFF-DESIGN PERFORMANCE OF SHOCK-IN-ROTOR  
TYPE SUPERSONIC BLADING

By Robert C. Graham, John F. Klapproth, and Frank J. Barina

Lewis Flight Propulsion Laboratory  
Cleveland, Ohio

CLASSIFICATION CHANGED  
UNCLASSIFIED

authority of *NACA Res Abs* *Effective*  
*RN-119* *Aug 16, 1957*

9-3-57

CLASSIFIED DOCUMENT

This document contains classified information affecting the National Defense of the United States within the meaning of the Espionage Act, USC 50-81 and 53. Its transmission or the revelation of its contents in any manner to an unauthorized person is prohibited by law.  
Information so classified may be imparted only to persons in the military and naval services of the United States, appropriate civilian officers and employees of the Federal Government who have a legitimate interest therein, and to United States citizens of known loyalty and discretion who of necessity must be informed thereof.

NATIONAL ADVISORY COMMITTEE  
FOR AERONAUTICS

WASHINGTON

May 7, 1951

NACA LIBRARY  
LANGLEY AERONAUTICAL LABORATORY  
Langley Field VA

CONFIDENTIAL

NACA RM E51C22



## NATIONAL ADVISORY COMMITTEE FOR AERONAUTICS

RESEARCH MEMORANDUM

## INVESTIGATION OF OFF-DESIGN PERFORMANCE OF SHOCK-IN-ROTOR

## TYPE SUPERSONIC BLADING

By Robert C. Graham, John F. Klapproth and Frank J. Barina

## SUMMARY

Results of a theoretical analysis of the off-design performance of shock-in-rotor type supersonic blades indicated that the losses associated with the external bow waves were only a small part of the over-all losses. It was found that throughout the off-design range studied, (entrance Mach numbers from 1.35 to starting) the greater share of the losses, other than viscous losses, can be attributed to the normal shock. An improvement in performance can be expected by reducing the normal shock losses through the introduction of a series of compression waves originating from the trailing surface of the blade prior to the actual passage entrance.

As in the case of the spiked diffuser, the compression is external, and the conventional contraction-ratio limits do not apply, thus permitting compression approaching isentropic.

## INTRODUCTION

In an attempt to extend the understanding of the operation of supersonic compressors at speeds less than design, a theoretical analysis has been made at the NACA Lewis laboratory of the flow process through supersonic blading over a range of entrance Mach numbers. The analysis is based on a shock-in-rotor type supersonic blading designed to have a passage-contained normal shock at design speed without an external-wave pattern.

The analysis provides an approximate evaluation of the losses, other than viscous losses due to the boundary layer, involved in flow through supersonic blading over a range of relative entrance Mach numbers from 1.35 to 1.65. The computed losses are assumed to be divided into two groups: normal-shock and external-wave losses.

Experimental verification of the analysis is provided by results obtained with a two-dimensional supersonic cascade. Over-all relative total-pressure recovery in the free stream is presented over a range of relative entrance Mach numbers from 1.47 to 1.65. A shadowgraph system was utilized to provide visual observation of shock waves, and pictures are presented at two relative entrance Mach numbers.

Based on the evaluation of the losses involved in the operation of supersonic blading at less than design entrance Mach numbers, design modifications are suggested that should result in an improvement in the performance within this range of operation.

### SYMBOLS

The following symbols are used in this report:

A	flow area
$A_1$	blade entrance area, $\frac{2\pi r}{n} \cos \beta_1$
$A_f$	effective flow area per blade
M	Mach number relative to blades
n	number of blades
P	total pressure relative to blades
$P_0$	relative total pressure before shock
$P_y$	relative total pressure after shock
$C_{r,B}$	blade contraction ratio, $A_1/A_2$
r	radius
V	velocity
y	coordinate measured perpendicular to relative free stream
$y_a$	origin of y coordinate
$y_b$	point of intersection between bow wave and last expansion wave from previous blade

$y_{SB}$  y coordinate of leading edge of blade  
 $a/y_{SB}$  constant, which is a function of free-stream Mach number only  
 $\alpha$  angle of attack,  $\beta_0 - \beta_1$   
 $\beta$  air-flow angle relative to blades measured from compressor axis  
 $\gamma$  ratio of specific heats, 1.4 for air  
 $\delta$   $\sqrt{M^2 - 1}$   
 $\rho$  density  
 $\varphi$  shock angle

Subscripts:

0 free-stream conditions  
1 station at blade entrance  
2 station at blade minimum section  
cr critical  
u tangential component of velocity  
z axial component of velocity

#### APPARATUS AND INSTRUMENTATION

The supersonic cascade used to obtain two-dimensional performance of the compressor blades investigated is shown in figure 1. Five two-dimensional passages are formed by the five blades and the upstream fairing block. The spillage passages (fig. 1(a)) are entirely separate from the main chamber so that it is possible to regulate the back pressure on the blades without affecting the pressure at the discharge of the nozzle.

The upper and lower window frames are fastened together through the two fairing blocks, and the five blades are held in position by pins through the upper and lower windows. The test-section assembly (fig. 1(b)) can be rotated relative to the nozzle-flow direction.

The upstream fairing block extends ahead of the line through the leading edge of the blades and effectively forms a sharp-edged flat plate. When this flat plate is parallel to the flow discharged from the nozzle, the Mach number entering the blades is equal to that at the nozzle discharge. When the test chamber is rotated and the fairing block placed at an angle of attack to the flow, there is an expansion or a compression around the fairing-block leading edge, which results in a change in Mach number and flow angle. The flow in passing through the disturbance becomes parallel to the fairing-block surface, so that the flow enters the blades at the design angle over the full Mach number range. Static-pressure taps are located on the fairing-block surface 1/2 inch downstream of the leading edge. In order to obtain the zero angle (and thus nozzle-discharge Mach number entering the blades), the test chamber is rotated until the static pressure on the fairing-block surface is equal to the static pressure at the nozzle discharge. Other Mach numbers, obtained by turning the test section, are determined by the pressure measurement, which checked the theoretical value obtained for the change in Prandtl-Meyer angle.

The cone-type combination probe used for the survey of total and static pressure at the discharge of the blades is shown in figure 1(c). The probe is mounted in an actuator that permits rotation and movement both in the spanwise direction and parallel to the trailing edges of the blades. A shadowgraph system is utilized to permit photographing the shock-wave formations in the passages.

#### ANALYSIS AND METHODS OF COMPUTATION

For the analysis of the operations of supersonic blading at speeds below design, a wave configuration as shown in figure 2 is assumed. The shock-wave pattern consists of a bow wave that is essentially normal to the flow at the passage entrance and asymptotically approaches the Mach angle. This wave is followed by an expansion of the flow around the leading edge of the blade. The assumed wave pattern is illustrated in figure 3, which is a shadowgraph of supersonic blades operating with a relative inlet Mach number below that which will allow starting.

At station 1, upstream of the wave pattern, the axial Mach number  $M_{z,0}$  and tangential Mach number  $M_{u,0}$  result in a relative air angle  $\beta_0$  that is larger than the design air-flow or blade angle  $\beta_1$  and a relative inlet Mach number  $M_0$  below the design value. The angle of attack  $\alpha$  is defined as  $(\beta_0 - \beta_1)$ .

The over-all losses in relative total pressure (neglecting viscous losses in the boundary layer) are assumed divided into two groups: (1) those associated with the external-wave system, and (2) the losses through the normal shock at the passage entrance.

With the assumption of an hyperbolic form for the bow wave as in reference 1, the shock angle  $\varphi$  at any point  $y/y_{SB}$  is

$$\varphi = \arctan \frac{\sqrt{\left(\frac{a}{y_{SB}}\right)^2 + \delta^2 \left(\frac{y}{y_{SB}}\right)^2}}{\delta^2 \left(\frac{y}{y_{SB}}\right)} \quad (1)$$

where  $a/y_{SB}$  is a constant, which is a function of the free-stream Mach number only,  $\delta$  is the cotangent of the Mach angle and is equal to  $\beta$  of reference 1, and  $y$  is a coordinate measured normal to the flow. In the two-dimensional case,  $y_{SB}$  is equal to the difference between the blade-entrance area  $A_1$  and the effective-flow area  $A_F$  (fig. 2).

The equation for total pressure recovery across a shock wave, which is given in reference 2 (p. 58), may be written in the form

$$\frac{P_y}{P_0} = \left( \frac{2\gamma}{\gamma+1} M^2 \sin^2 \varphi - \frac{\gamma-1}{\gamma+1} \right)^{\frac{1}{1-\gamma}} \left( \frac{\gamma-1}{\gamma+1} \frac{M^2 \sin^2 \varphi + 2}{M^2 \sin^2 \varphi} \right)^{\frac{\gamma}{1-\gamma}} \quad (2)$$

where  $\varphi$  is the shock angle obtained from equation (1).

The loss in relative total pressure due to the bow wave (reference 3) may be written as

$$\left( 1 - \frac{P_1}{P_0} \right) = \frac{y_{SB}}{\frac{2\pi r}{n} \cos \beta_1} \int_0^\infty \left( 1 - \frac{P_y}{P_0} \right) d\left(\frac{y}{y_{SB}}\right) \quad (3)$$

where the term  $\frac{y_{SB}}{\frac{2\pi r}{n} \cos \beta_1}$  of equation (3) is equal to  $\frac{A_1 - A_f}{A_1}$ . The

term  $\int_0^{\frac{y}{y_{SB}}} \left(1 - \frac{P_y}{P_0}\right) d\left(\frac{y}{y_{SB}}\right)$ , when evaluated over the range of  $y/y_{SB}$

from zero to infinity is a function of relative Mach number only, and is presented in figure 4.

In order to compute the flow losses in the bow wave, the value of

$\int_0^{\infty} \left(1 - \frac{P_y}{P_0}\right) d\left(\frac{y}{y_{SB}}\right)$  is taken at the entrance Mach number  $M_1$  rather

than at the free stream  $M_0$ . The use of  $M_1$  can be justified by the examination of the losses along a single bow wave. A plot of

$\int_0^{\frac{y}{y_{SB}}} \left(1 - \frac{P_y}{P_0}\right) d\left(\frac{y}{y_{SB}}\right)$  for a Mach number  $M_1$  of 1.40 is presented in

figure 5. For the blade form used in the investigation and for operation at an entrance Mach number  $M_1$  of 1.40, point  $y_a$  of figure 2 corresponds to a  $y/y_{SB}$  value of zero and point  $y_b$  to a  $y/y_{SB}$  value of approximately 20. Point  $y_b$  represents the point of intersection of the last expansion with the bow wave, and therefore, the Mach number upstream of the shock from  $y_a$  to  $y_b$  is essentially constant. Inasmuch as the losses that result from this section of the bow wave represent about 97 percent of the total losses along the entire wave, the entrance Mach number  $M_1$  is used for the evaluation of shock recovery for the full range of  $y/y_{SB}$ . A similar distribution of losses along the bow wave was found over the full range of Mach numbers investigated.

For a given blade geometry and free-stream Mach number, the characteristics of the flow entering a blade passage can be evaluated by use of the continuity equation. The free-stream flow and the flow through the minimum section may be equated as follows:

$$\rho_0 V_0 \cos \beta_0 \frac{2\pi r}{n} = \rho_2 V_2 \frac{\cos \beta_1}{C_{r,B}} \frac{2\pi r}{n} \quad (4)$$

If it is assumed that the minimum section will flow full at sonic velocity, equation (4) can be written as

$$\frac{\cos \beta_0}{\frac{P_2}{P_0}} = \frac{A_0}{A_{cr}} \frac{\cos \beta_1}{C_{r,B}} \quad (5)$$

The blade contraction ratio  $C_{r,B}$  and the blade angle  $\beta_1$  are defined by the blade geometry. The critical-area ratio  $A_{cr}/A$ , a function of the assigned free-stream Mach number, is given in reference 2 (p. 34) and can be put in the form

$$\left(\frac{A}{A_{cr}}\right)^2 = \frac{1}{M^2} \left[ \frac{2}{\gamma+1} \left( 1 + \frac{\gamma-1}{2} M^2 \right) \right]^{\frac{\gamma+1}{\gamma-1}} \quad (6)$$

where  $A_{cr}$  is identical with  $A^*$  of reference 2 and represents the condition at the throat at a Mach number of 1.

Computation of the flow involves a trial-and-error determination of the free-stream flow angle  $\beta_0$  and the associated over-all total-pressure recovery  $P_2/P_0$  that satisfies equation (5) for a given free-stream Mach number  $M_0$ .

The computation requires the assumption of a free-stream flow angle. The flow is assumed to expand around the angle of attack, which results in a Mach number upstream of the normal shock  $M_1$  slightly higher than  $M_0$ . The first approximation of the losses is obtained from  $M_1$  and the area ratio  $\frac{A_1 - A_f}{A_1}$  by use of equation (3). By using the losses thus computed, a corrected  $M_1$  is determined. The losses and  $M_1$  are reiterated until there is no further change in  $M_1$ . Three approximations were found adequate. The over-all total-pressure recovery  $P_2/P_0$  is the product of the bow-wave recovery (from equation (3)) and the normal-shock recovery (from equation (2) using the corrected final  $M_1$  and  $\phi = 90^\circ$ ). The assumed free-stream flow angle and the resulting over-all recovery are revised until the ratio  $\frac{\cos \beta_0}{\frac{P_2}{P_0}}$  satisfies equation (5).

$$\frac{P_2}{P_0}$$



The theoretical over-all recovery of the free stream, made up of wave recovery and normal-shock recovery (neglecting viscous effects along the blade), can be plotted as a function of relative inlet Mach number for any given set of blading. These recovery curves for the particular supersonic blades being investigated are presented in figure 6. It is evident that the bow-wave losses are of a considerably smaller magnitude than the normal-shock losses over the range of Mach numbers from 1.35 to starting. At a free-stream Mach number of 1.635 the bow wave becomes attached and a passage-contained shock configuration is established. The bow-wave losses approach zero as the wave approaches attachment, and after starting there is a sharp reduction in normal-shock losses due to the contraction in the supersonic portion of the passage.

#### EXPERIMENTAL RESULTS

Shown also in figure 6 is the over-all total-pressure recovery as determined from the experimental investigation. Midpassage-exit total pressure was used in the computation of recovery, and therefore the only losses included in the experimental data, but omitted in the theoretical recovery, are those due to the secondary shocks in the passage. These shocks exist in a region of low supersonic velocities and therefore midstream losses other than those theoretically accounted for should be small.

Difficulty arises when an attempt is made to correlate accurately the experimental conditions with an equivalent theoretical condition. After the supersonic flow has been established in the blading, the entrance Mach number can be determined from static-pressure measurements on the upstream fairing block. For unstarted flow, this method should be reasonably accurate when the external wave pattern from the blade does not intersect the oblique shock used to establish the entrance flow, as is the case shown in figure 3. In attempting to obtain lower inlet Mach numbers, however, the bow wave intersected the oblique shock wave, making the determination of an equivalent far upstream Mach number impossible by use of the static pressures on the fairing block. Consequently, the equivalent entrance Mach numbers for experimental observations below 1.53 may be in error by several percent.

It was impossible to determine accurately the Mach number upstream of the normal shock by measuring weak oblique shock angles; and it was difficult therefore to obtain experimental verification of the division of the over-all total-pressure loss. Estimations of the normal-shock losses from the oblique shock angles measured on a series of pictures

indicate, however, that the theoretical values shown in figure 6 are of the correct order of magnitude. For example, the measurement of angles in figure 3 gives a range of Mach numbers preceeding the normal shock at the passage entrance from 1.52 to 1.64 depending upon the particular wave selected. This range would result in a normal-shock-recovery range from 0.88 to 0.92, whereas the theoretical value is 0.895.

A shadowgraph of the flow conditions after starting is presented in figure 7. This picture represents a maximum back-pressure condition for started flow and it is evident that the design passage-contained normal shock was not established, but was replaced by a series of weak compressions. The total-pressure recovery is therefore higher than the theoretical value.

#### DISCUSSION

The losses resulting from an external-wave pattern are only a small part of the total losses (fig. 6). Any design modification that would result in a reduction of the normal-shock losses would therefore cause an equivalent increase in over-all total-pressure recovery. In order to improve the normal-shock recovery, the Mach number ahead of the shock must be reduced. This softening of the shock could be accomplished by the introduction of a series of compression waves originating from the trailing surface of the blade prior to the actual blade entrance. The addition of these external compression waves would be analogous to the spiked diffuser and should essentially eliminate the discontinuity in the recovery curves presented in figure 6.

It is interesting to note that when the compression is outside of the confined passage, as in the case of the spiked diffuser, conventional contraction-ratio limitations would not be applicable, and a compression approaching isentropic could be obtained. This ability to decelerate the flow to a velocity close to sonic before the normal shock would result in an even greater improvement in normal-shock recovery, and thus over-all total-pressure recovery.

#### SUMMARY OF RESULTS

The following results were obtained from a theoretical analysis of the off-design performance of shock-in-rotor type supersonic blading:

1. The losses resulting from the external-wave pattern of supersonic blading operating below the starting speed were small in comparison to the over-all losses.

2. It was indicated that in the range of relative entrance Mach numbers from 1.35 to starting (1.64), the largest losses can be attributed to the normal shock.

3. The normal-shock losses can be reduced by the introduction of external compression waves originating from the trailing surface of the blade upstream of the actual blade entrance.

4. Inasmuch as the compression waves, as in the case of the spiked diffuser, are not confined within the passage, the conventional contraction-ratio limitations do not apply; in fact, the compression could approach isentropic.

Lewis Flight Propulsion Laboratory,  
National Advisory Committee for Aeronautics,  
Cleveland, Ohio.

#### REFERENCES

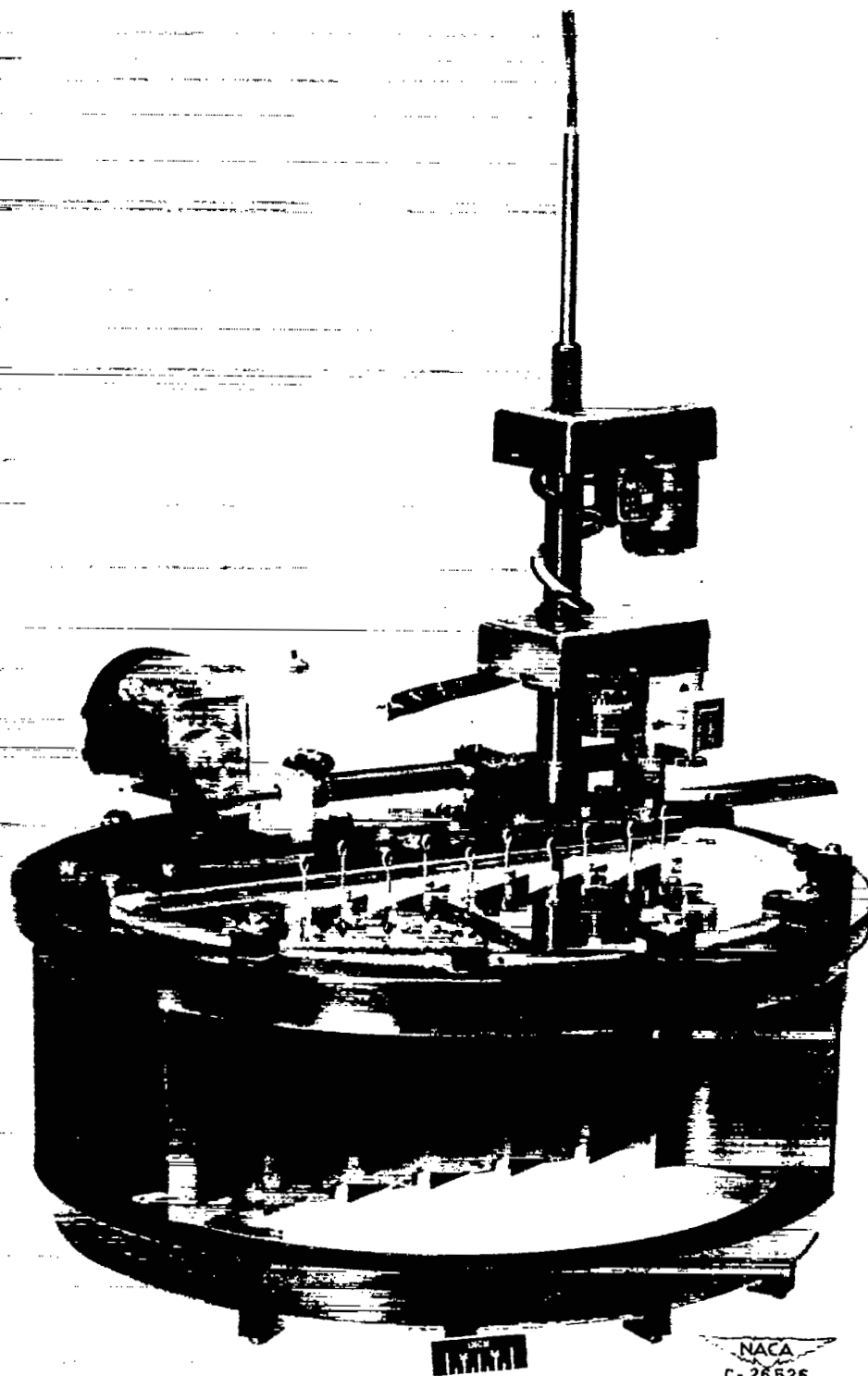
1. Moeckel, W. E.: Approximate Method for Predicting Form and Location of Detached Shock Waves Ahead of Plane or Axially Symmetric Bodies. NACA TN 1921, 1949.
2. Liepmann, Hans Wolfgang, and Puckett, Allen E.: Introduction to Aerodynamics of a Compressible Fluid. John Wiley & Sons, Inc., 1947.
3. Klapproth, John F.: Approximate Relative-Total-Pressure Losses of an Infinite Cascade of Supersonic Blades with Finite Leading-Edge Thickness. NACA RM E9L21, 1950.



(a) Test chamber.

Figure 1. Supersonic cascade investigated.

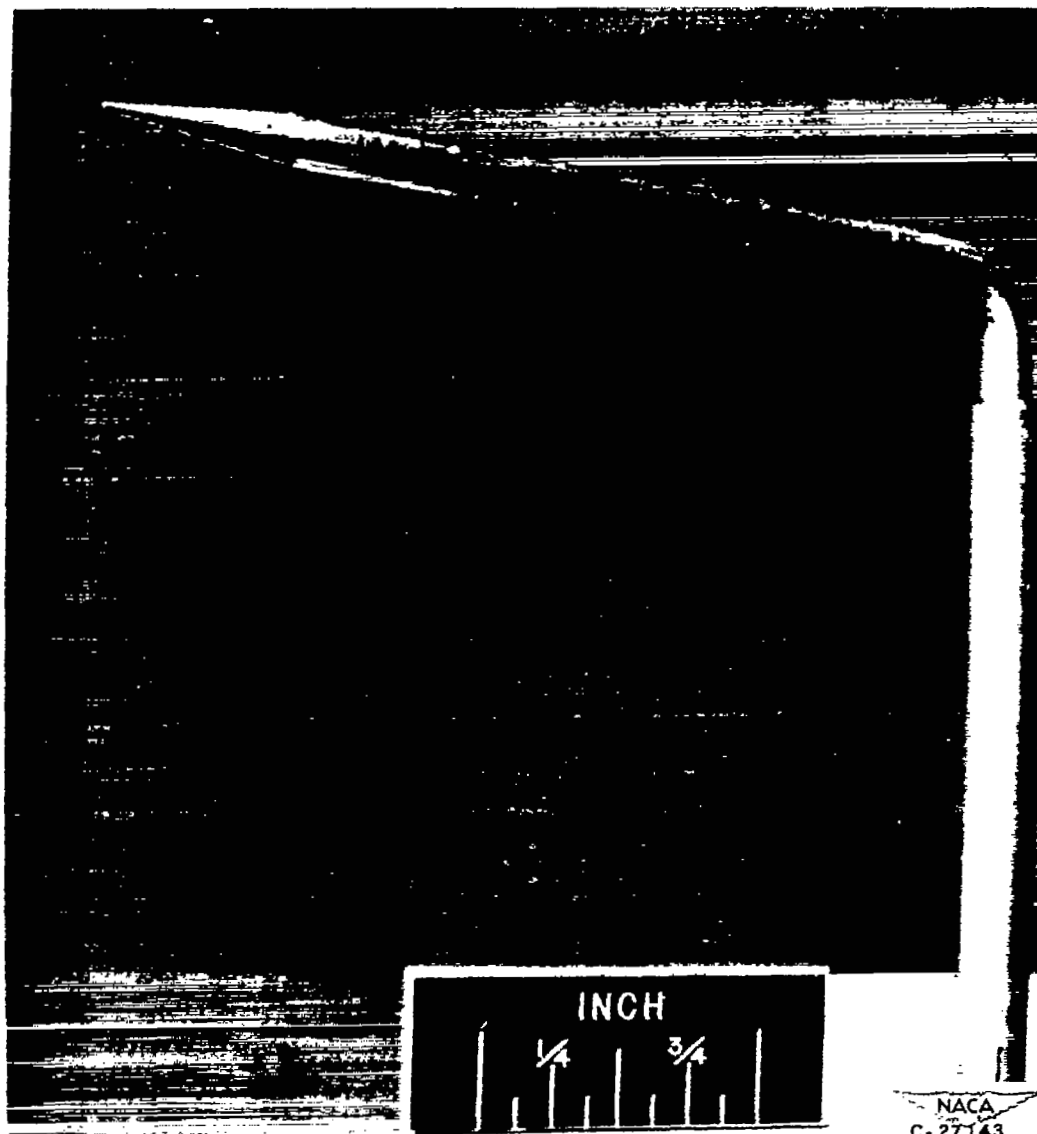




(b) Test section.

Figure 1. - Continued. Supersonic cascade investigated.





(c) Cone-type combination survey probe.

Figure 1. - Concluded. Supersonic cascade investigated.





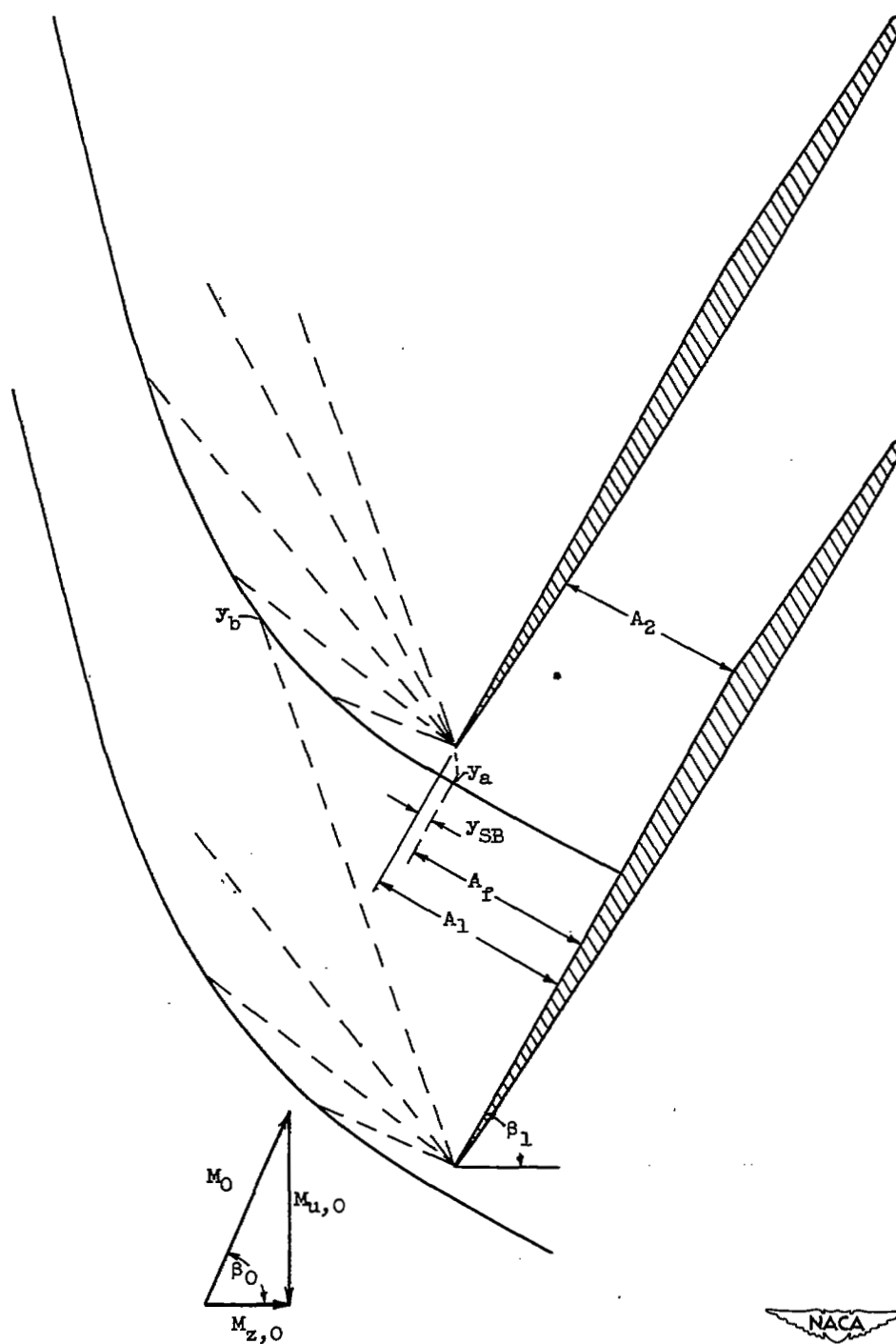


Figure 2. - Assumed wave configuration of supersonic blading at off-design speed.





Figure 3. - Shadowgraph picture of cascade of unstarted supersonic blades.

NACA  
C-27176



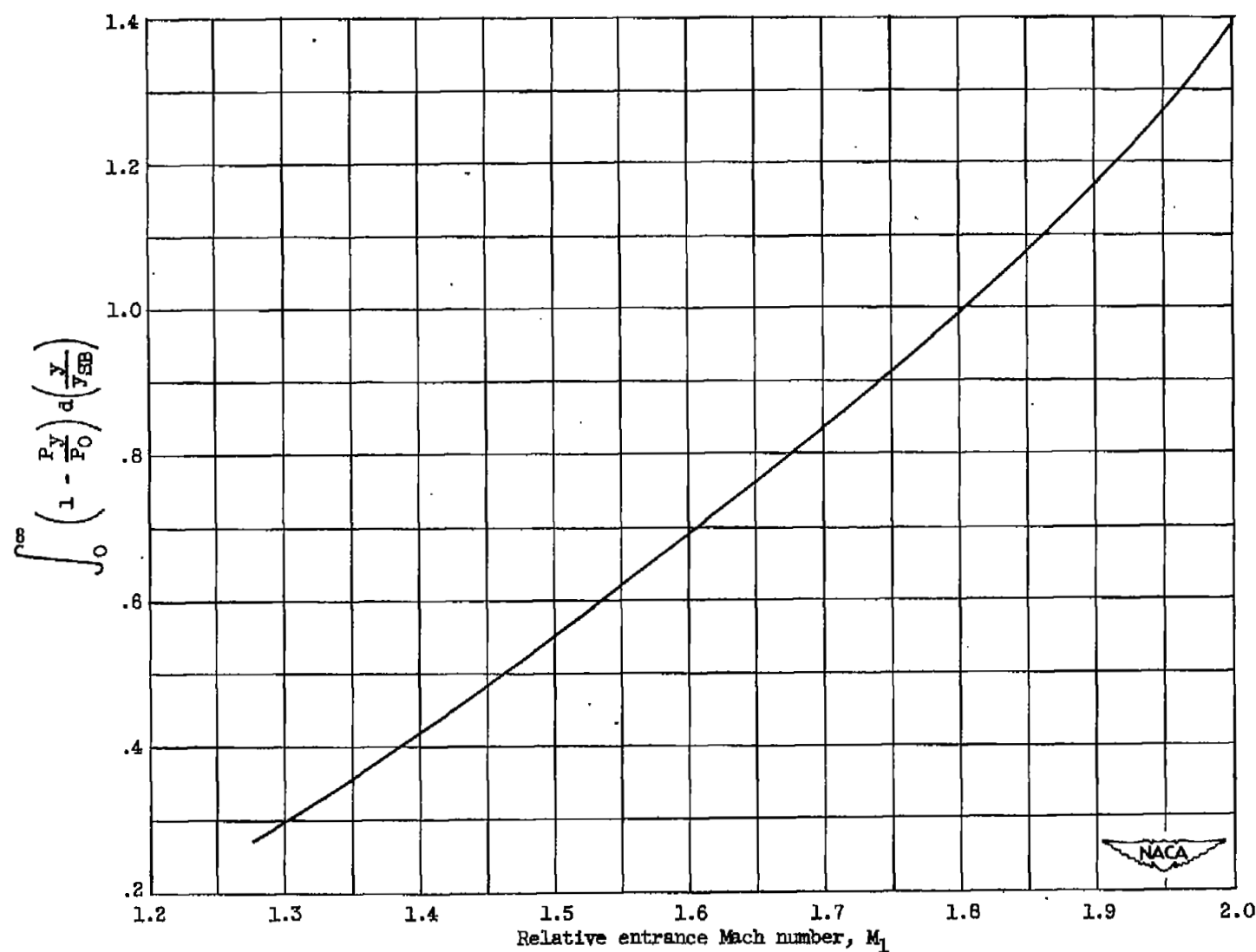


Figure 4. - Loss function along standing bow wave.

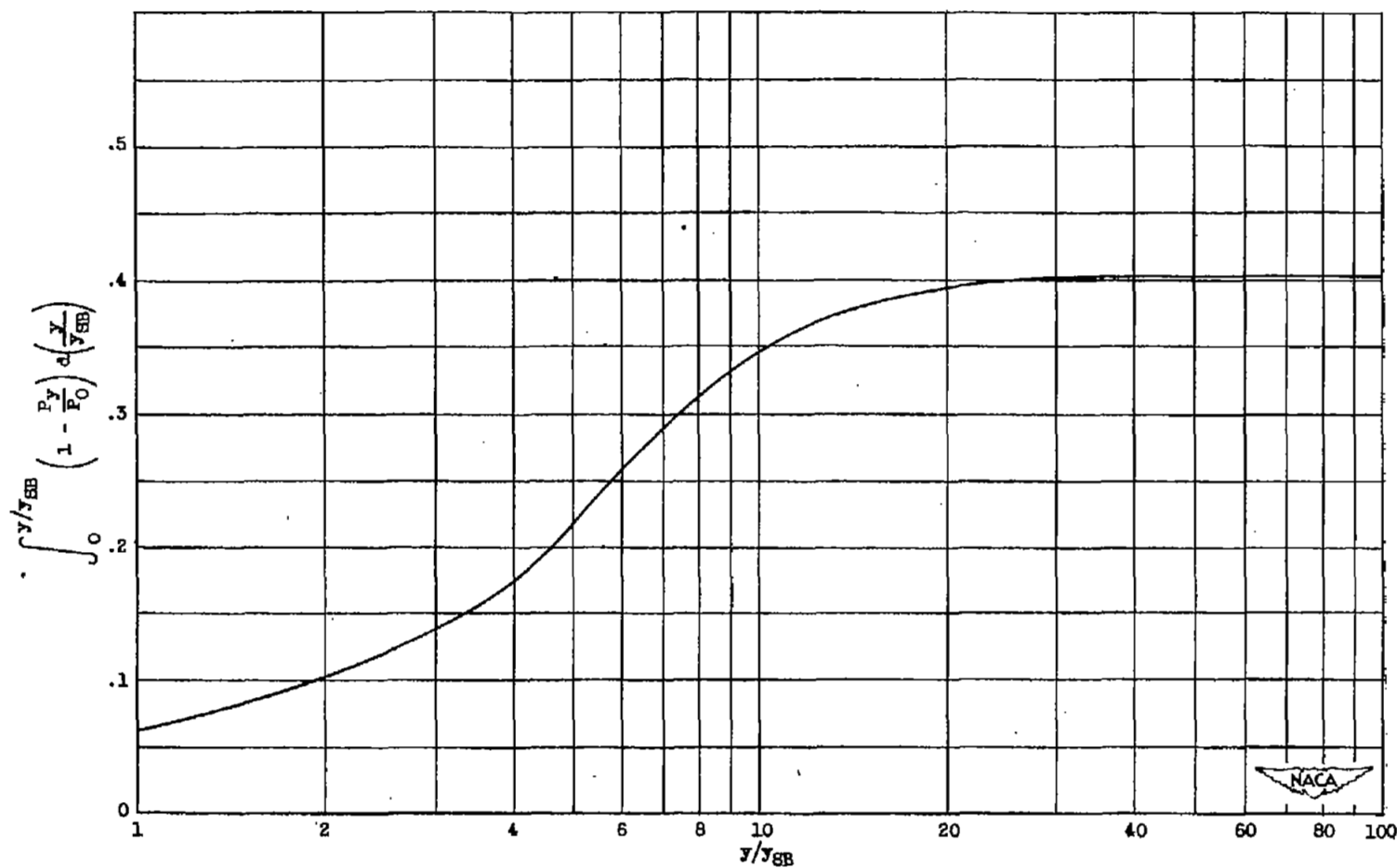


Figure 5. - Distribution of losses along bow wave at relative entrance Mach number  $M_1$  of 1.40.

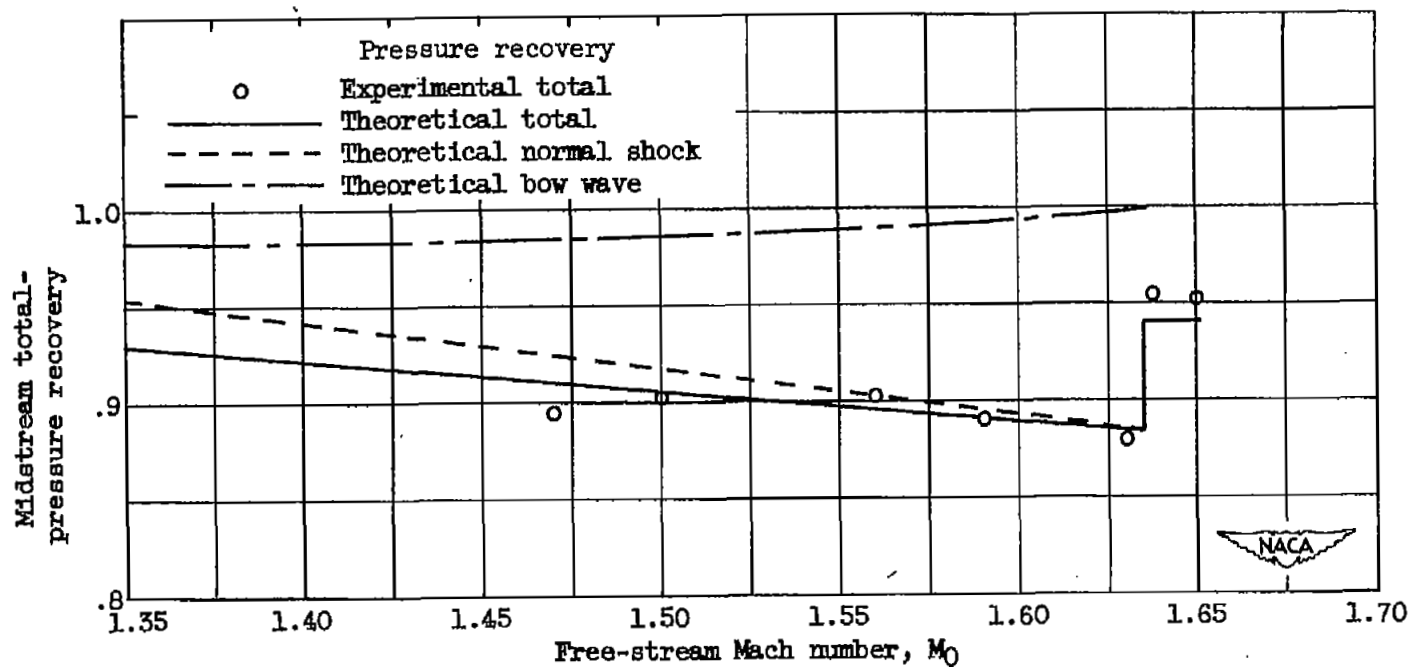


Figure 6. - Theoretical and experimental relative total-pressure recovery.





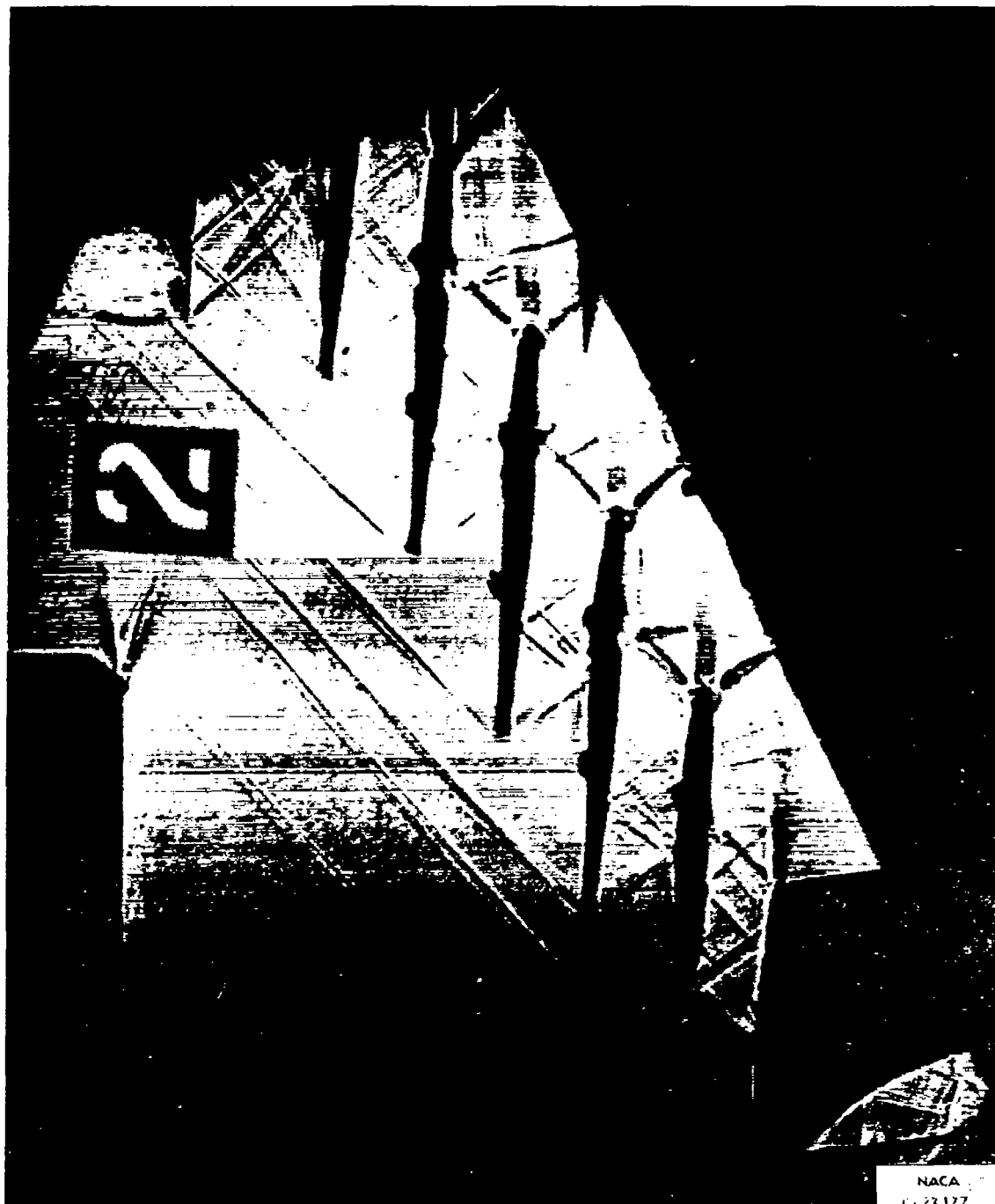


Figure 7. - Shadowgraph picture of cascade of started supersonic blades.

NASA Technical Library



3 1176 01435 2257